

EEG functional connectivity and deep learning for automatic diagnosis of brain disorders: Alzheimer’s disease and schizophrenia

Caroline L. Alves^{*,1,2,*}, Aruane M. Pineda^{2,†}, Kirstin Roster², Christiane Thielemann¹ and Francisco A. Rodrigues²

¹*BioMEMS, Technische Hochschule Aschaffenburg, Aschaffenburg, Germany*

²*Universidade de São Paulo (USP),*

Instituto de Ciências Matemáticas e de Computação, São Carlos, SP, Brazil

Mental disorders are among the leading causes of disability worldwide. The first step in treating these conditions is to obtain an accurate diagnosis, but the absence of established clinical tests makes this task challenging. Machine learning algorithms can provide a possible solution to this problem, as we describe in this work. We present a method for the automatic diagnosis of mental disorders based on the matrix of connections obtained from EEG time series and deep learning. We show that our approach can classify patients with Alzheimer’s disease and schizophrenia with a high level of accuracy. The comparison with the traditional cases, that use raw EEG time series, shows that our method provides the highest precision. Therefore, the application of deep neural networks on data from brain connections is a very promising method to the diagnosis of neurological disorders.

I. INTRODUCTION

Neurological disorders, including Alzheimer’s disease (AD) and schizophrenia (SZ), are among the main priorities in the present global health agenda [1]. AD is a type of dementia that affects primarily elderly individuals and is characterized by the degeneration of brain tissue, leading to impaired intellectual and social abilities [2]. Currently, around 25 million people live with AD [3]. In the US, nearly six million individuals are affected by AD, with incidence projected to increase more than two-fold to 13.8 million by 2050 [4]. Individuals with SZ have symptoms such as hallucinations, incoherent thinking, delusions, decreased intellectual functioning, difficulty in expressing emotions, and agitation [5, 6]. According to the World Health Organization (WHO), SZ affects around 26 million people worldwide [7].

The base for a successful treatment of AD and SZ is the correct diagnosis. However, in the absence of established clinical tests for neurological disorders, both the diagnosis and the determination of the stage of AD and SZ are based primarily on qualitative interviews, including psychiatric history and current symptoms, and the assessment of behaviour. These observations may be subjective, imprecise, and incomplete [8–10]. To provide a quantitative evaluation of mental disorders, methods based on Magnetic Resonance Imaging (MRI), Computerized Tomography (CT) [11], and Positron Emission Tomography (PET) [12, 13] has been used to aid professionals in the diagnostic process [14]. However, the use of multiple imaging devices can be expensive to implement and the fusion of images from different devices can have poor quality due to motion artifacts.

To overcome these restrictions, EEG data is a viable candidate to support the diagnosis of SZ and AD [15]. Although EEG has a low spatial resolution, it has a compar-

atively low cost, good temporal resolution and is easily available in most contexts. Nonetheless, visual analysis of EEG data is time-consuming, requires specialized training, and is error-prone [16–18]. However, we can consider automatic evaluation of EEG time series using modern classification algorithms, which can help to improve the efficiency and accuracy of AD and SZ diagnosis, as verified in previous works [19–22].

Moreover, instead of using raw EEG time series, it is possible to encompass the connections between brain regions by constructing cortical complex networks [23]. In this case, we build cortical networks for healthy and individuals with neurological disorders. To distinguish between them, we use network measures to describe the network structure, as described in a previous work of ours [24] (see also [25, 26] for a description of the methodology used in network classification). Therefore, each network is mapped into a d dimensional space, where d is the number of measures adopted for network characterization. This process of building a set of features to represent the input data is called feature engineering. After extracting the network features for the two classes of networks, i.e. healthy and individuals with mental disorders, supervised learning algorithms are adjusted to perform automatic classification. Previous works verified that this approach enables the diagnosis with accuracy higher than 80% in the case of childhood-onset schizophrenia [24].

Although this methodology has been used for many different diseases (e.g. [19, 24, 27]) the performance of the algorithm depends on the measures selected to describe the network structure. The network properties included in the model could represent just a subset of the information necessary to get the best performance of the supervised model. Therefore, the network representation can be incomplete, restricting the accuracy of the classifiers. One possible solution to this problem is the use of a matrix of connections in combination with and deep neural networks [28], as we show in the present paper. In this case, instead of extracting the network measures, the matrix of connections is considered as input to train

* caroline.alves@th-ab.de

† aruane.pineda@usp.br

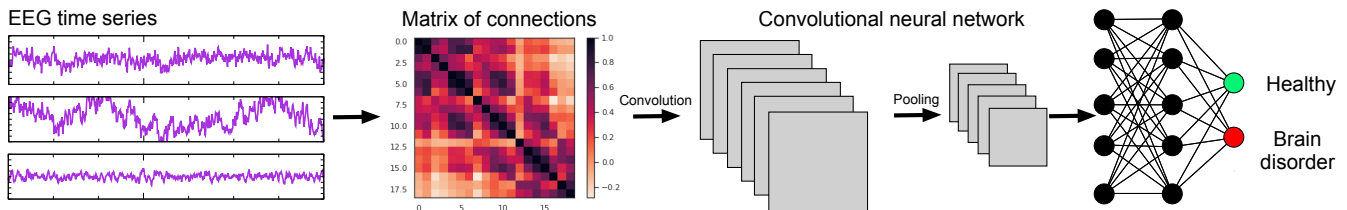


FIG. 1. Illustration of the method for automatic diagnosis of mental disorders based on EEG time series. Time series are collected and the correlation between electrodes are calculated yielding the matrices of connections, which encompass the functional connectivity between brain regions. Finally, the CNN is adjusted to enable the automatic classification of individuals.

a deep neural network. This matrix encodes all the information necessary to represent the network structure and avoid the choice of network measures.

Therefore, we consider the matrix of connections between brain areas and deep neural networks to distinguish individuals with AD and SZ from healthy controls. Other than previous works, where only raw time series are adopted as input for the neural network [29–35], we do not ignore the connections between the electrodes used to record the time series. We construct the matrix of connections by using Granger causality, Pearson’s and Spearman’s correlations [36–38]. We verify that this information about the connections is fundamental and improves the classification, compared to the previously mentioned approaches that use only raw EEG time series.

In summary, in this work we achieve the following contributions:

- We propose a method to classify EEG time series from healthy and patients presenting AD and SZ. With a matrix of connections as input for a tuned Convolutional Neural Network (CNN) model, the accuracy obtained is close to 100 % for both disorders. Our results are more accurate than those observed in previous works that consider only raw EEG time series, reinforcing the importance of the network structure on the diagnosis of mental disorders.
- We show that the method to infer the matrices of connections influences the quality of the classification results. For SZ, the Granger causality provides the most accurate classification, whereas, for AD, the Pearson’s correlation yields the highest accuracy.
- Our framework is general and can be used in EEG data from any brain disorder. It allows to determine the best cortical network representation and adjust the CNN to optimize the accuracy.

In the next sections, we outline the data set, present the CNN architecture and show our results, comparing them with more common approaches that do not consider the connections between brain areas.

II. EEG DATA

The AD data set considered here is composed of EEG time series recorded at a sampling frequency of 128 Hz and a duration of eight seconds for each individual and at 19 channels (F_{p1} , F_{p2} , F_7 , F_3 , F_z , F_4 , F_8 , T_3 , C_3 , C_z , C_4 , T_4 , T_5 , P_3 , P_z , P_4 , T_6 , O_1 , and O_2) [19, 39]. The letters F, C, P, O, and T refer to the respective cerebral lobes frontal (F), central (C), parietal (P), occipital (O), and temporal (T). The data is divided into two sets. The first one consists of 24 healthy elderly individuals (control group; aged 72 ± 11 years) who do not have any history of neurological disorders. The second one is made of 24 elderly individuals with AD (aged 69 ± 16 years) diagnosed by the National Institute of Neurological and Communicative Disorders and Stroke, the Alzheimer’s Disease and Related Disorders Association (NINCDS-ADRDA), following the Diagnostic and Statistical Manual of Mental Disorders (DSM)-III-R criteria ([19, 39]).

The data set used for diagnosis of SZ can be found at [40]. This data contains 16-channel EEG time series recorded at a sampling frequency of 128 Hz over one minute, including F_7 , F_3 , F_4 , F_8 , T_3 , C_3 , C_z , C_4 , T_4 , T_5 , P_3 , P_z , P_4 , T_6 , O_1 , and O_2 . Notice that both data set come from studies of 16 common brain regions, with the AD data set having three more regions analyzed. Furthermore, it also includes two sets, (i) one of 39 healthy young individuals (control group; aged 11 to 14 years) and (ii) one of 45 teenagers individuals (aged 11 to 14 years) with symptoms of schizophrenia.

III. CONCEPTS AND METHODS

Our framework to perform the automatic diagnosis of AD and SZ is illustrated in Figure 1. In a first step, EEG time series, which are free of artifacts, are used to construct the matrices of connections. The strength of the connections between two brain regions is quantified by three different methods: (i) Granger causality test [41], (ii) the Pearson’s [42] and (iii) Spearman’s [43] correlation measures. For Granger causality, a statistical hypothesis test is done and p-values are obtained. The matrices are filled with “1” if $p < 0.05$ and “0” if $p \geq 0.05$.

Matrices are calculated for AD data sets (19 EEG channels) and for SZ data sets (16 EEG channels). These matrices are inserted in a CNN to discriminate healthy individuals from individuals diagnosed with AD and SZ (see Figure 1). Notice that the use of different methods to infer the brain areas is necessary because there is no general method to infer functional connectivity [36–38, 44]. Indeed, choosing the best metric to infer these connections between brain areas is a current challenge in network neuroscience (e.g. [45, 46]).

A. Convolutional Neural Network

CNN is a type of neural network [47] with three types of layers and masked parameters, as proposed in [48, 49]. The convolutional layer performs the mathematical operation called convolution, which is done in more than one dimension at a time. The weights of the artificial neurons are represented by a tensor called kernel (or filter). The outputs from the convolutional layer include the main features from the input data. The convolution process between neurons and kernels produces outputs called feature maps.

The pooling layer reduces the dimensionality and operates similarly to the convolutional layer. The difference is that pooling kernels are weightless and add aggregation functions to their input data, such as a maximum or mean function [50, 51]. The max pooling function is used here to return the highest value within an area of the tensor, which reduces the size of the feature map. The fully connected layer categorizes input data into different classes, based on an initial set of data used for training. The artificial neurons in the max pooling and fully connected layers are connected, as the output predicts precisely the result of the input EEG data as healthy and unhealthy [20].

Two approaches for the CNN architectures are proposed here, one using a tuning method (CNN_{tuned}) and another without this optimization step (CNN_{untuned}). Tuning is an optimization method used to find the values of hyperparameters to improve the performance of the CNN model [52]. Three tuning techniques are used in the present work: (i) random search [53], (ii) hyperband [54] and (iii) Bayesian optimization [55]. The traditional way to optimize the hyperparameters is exhaustive searching through a manually specified parameters search space and evaluate all possible combinations of these parameter values. However, this approach has a high computational cost. An alternative method is to select the values of parameters in the search space at random until maximize the objective function (here, this objective function is the maximization of accuracy).

The idea of hyper-band optimizations is to select different possible models (with different hyperparameters values), train them for a time, and discard the worst one at each iteration, until a few combinations remain. In contrast, Bayesian optimization is a global optimization

method that uses the Bayes Theorem to direct the search to find the minimum or maximum of a certain objective function [28].

In the CNN_{tuned} model, the dropout regularization technique is employed to avoid overfitting [56]. The layers and range used for hyperparameters are presented in table I. The best CNN_{tuned} architectures tuned for each data set individually are depicted in table II. The CNN_{untuned} model presents fewer layers and therefore lower computational costs. The parameters used in our analysis are described in table III.

B. Evaluation

Since we have a two-class classification problem (negative and positive), we consider the precision and recall measures in the evaluation process [57]. Precision (also called specificity) corresponds to the hit rate in the negative class, whereas recall (also called sensitivity) measures how well a classifier can predict positive examples (hit rate in the positive class). For visualization of these two measures, the receiver operating characteristic (ROC) curve is a common method as it displays the relation between the rate of true positives and false positives. The area below this curve, called area under ROC curve (AUC) has been widely used in classification problems [58], mainly for medical diagnoses [59–62]. The value of the AUC varies from 0 to 1, where the value of one corresponds to a classification result free of errors. $AUC = 0.5$ indicates that the classifier is not able to distinguish the two classes — this result is equal to the random choice. Furthermore, we consider the micro average of ROC curve, which computes the AUC metric independently for each class (calculate AUC metric for healthy individuals, class zero, and separately calculate for unhealthy subjects, class one) and then the average is computed considering these classes equally. The macro average is also used in our evaluation, which does not consider both classes equally, but aggregates the contributions of the classes separately and then calculates the average.

IV. RESULTS AND DISCUSSION

We consider the EEG time series described in section II to construct the matrices of connections for healthy controls and individuals diagnosed with AD and SZ, following the description in section III. These matrices are built by using the Granger causality test, Pearson’s and Spearman’s correlations measures for both data sets. In Figures 2 and 3, some examples of such matrices of connections are showed and differences between them can be noticed visually in both cases.

The matrices of connections are inserted into the CNN by applying the flattening method, which converts the data into a 1-dimensional array that is input to the

TABLE I. Best hyperparameters and layer configurations obtained for the CNN_{tuned} model.

Type of Layer	Tuning hyperparameter	Value
Convolutional	—	—
Convolutional	dropout	[0.00, 0.05, 0.10, 0.15, 0.20, 0.25, 0.30, 0.35, 0.40, 0.45, 0.50]
Convolutional	—	—
Convolutional	number of filters	[32, 64]
Max Pooling	dropout	[0.00, 0.50, 0.10, 0.15, 0.20]
Flatten	—	—
Dense	- units	[32, 64, 96...512]
	-activation	[relu, tanh, sigmoid]
Dropout	rate	[0.00, 0.50, 0.10, 0.15, 0.20]
Adam optimization	learning rate	$min - value = 1e^{-4}$
compile	rate	$max - value = 1e^{-2}$
		sampling= LOG

TABLE II. The network architecture for the CNN_{tuned} model used in the AD and SZ data sets.

Type of Layer	Output Shape (AD)	Output Shape (SZ)	Parameter
Convolutional	(None, 17, 17, 16)	(None, 14, 14, 16)	160
Convolutional	(None, 15, 15, 16)	(None, 12, 12, 16)	2320
max-pooling	(None, 7, 7, 16)	(None, 6, 6, 16)	0
dropout	(None, 7, 7, 16)	(None, 6, 6, 16)	0
Convolutional	(None, 5, 5, 32)	(None, 4, 4, 32)	4640
Convolutional	(None, 3, 3, 32)	(None, 2, 2, 32)	9248
max-pooling	(None, 1, 1, 32)	(None, 1, 1, 32)	0
dropout	(None, 1, 1, 32)	(None, 1, 1, 32)	0
flatten	(None, 32)	(None, 32)	0
dense	(None, 160)	(None, 160)	5280
dropout	(None, 160)	(None, 160)	0
dense	(None, 2)	(None, 2)	3

next layer. Two CNN architectures are considered, i.e. CNN_{tuned} and CNN_{untuned}, to evaluate the classification. The CNN_{tuned} is obtained by hyperparameter optimization, whereas the CNN_{untuned} is a simpler model, without using the tuning optimization. The evaluation of both models is done by using the area under the ROC curve (AUC). Nested k-fold cross-validation ($k = 10$) for model selection, adjustment and evaluation is considered here.

The results for the CNN_{tuned} model is shown in tables IV and V, for AD and SZ, respectively. In all the cases, the CNN_{tuned} model can unambiguously distinguish healthy individuals from individuals diagnosed with a brain disorder. The best results with an accuracy close to 100% are obtained for both AD and SZ in the testing set using random search for hyperparameter tuning.

Concerning the CNN_{untuned} model, the results are shown in tables VI and VII for AD and SZ, respectively. For the AD data set, the best results are found using Pearson’s correlation with a test accuracy of 92%. Regarding SZ disease, independently of the method used for the construction of the matrices of connections, results

are close to the random guessing (see table VII). Therefore, the CNN_{tuned} model is more accurate for both AD and SZ diagnosis.

Importantly, the overall predictive performance depends on the choice of measure to construct the matrices of connections. In the case of AD, Pearson’s correlation provides the best performance in CNN_{tuned} (see table IV). On the other hand, in the case of SZ, Granger causality is superior to the other methods (see table V). Therefore, there is no general method to infer the connections and obtain the most accurate results. Thus, different methods should be considered to develop an accurate framework for the automatic diagnosis of mental disorders.

For a comparison of our method with the more common approach known from the literature, the classification is performed by applying the raw EEG time series as input for the CNN_{tuned} model (whose performance is the best for both diseases, as discussed before). The results are shown in tables VIII and IX for AD and SZ, respectively. The accuracy of 75% for AD and 55% for SZ are obtained. This outcome is supported by results available in the literature. Janghel and Rathore [63] ob-

TABLE III. The network architecture for the CNN_{untuned} model used in the AD and SZ data sets.

Type of Layer	Output Layer (AD)	Output Layer (SZ)	Kernel
Input Layer	19 x 19 x 1	16x16x1	-
Convolution	18 x 18 x 32	15 x 15 x 32	4
Max pooling	18 x 18 x 32	15 x 15 x 32	2
Convolution	17 x17 x 16	14 x 14 x 16	4
Max pooling	17 x17 x 16	14 x 14 x16	2
Flatten	17 x17 x 16	3136	-
Fully connected	10	10	-
Fully connected	1	1	-

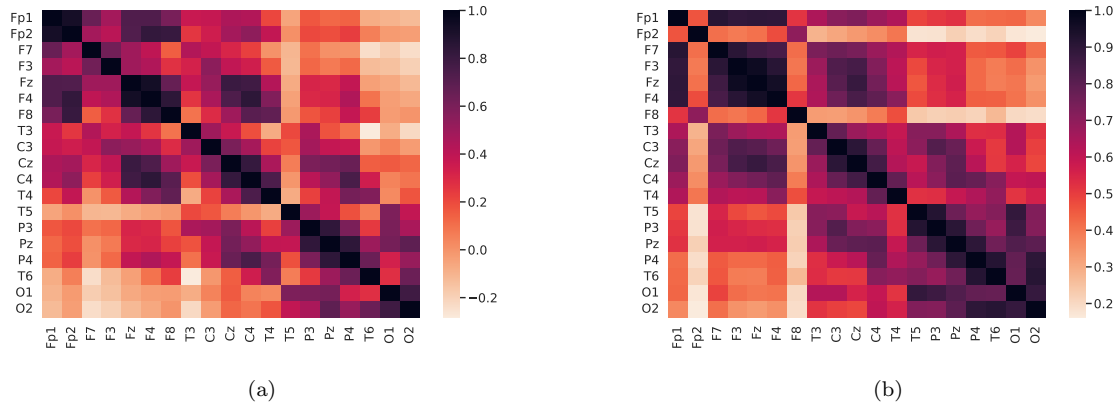


FIG. 2. Example of matrices of connections calculated with Pearson's correlation for (a) an individual with diagnosed AD and (b) an healthy individual.

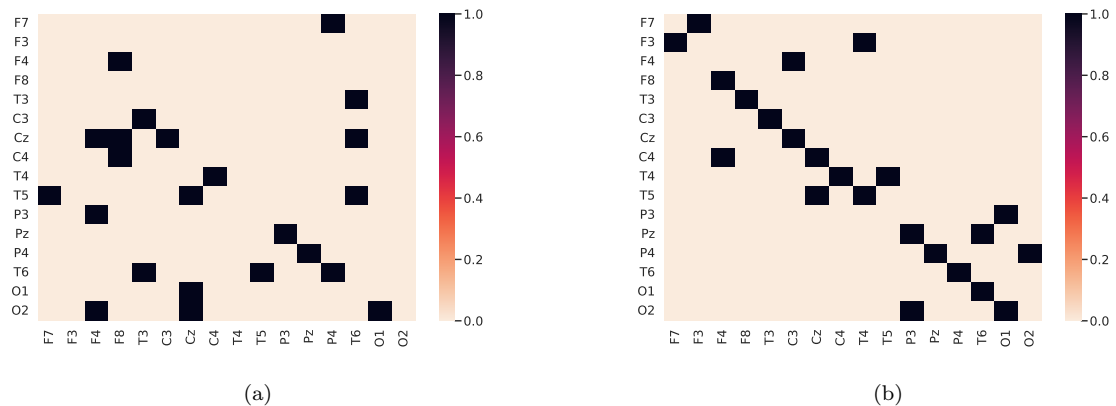


FIG. 3. Example of matrices of connections calculated with Granger causality test for (a) an individual with diagnosed SZ and (b) an healthy individual.

tained an accuracy of 76% for AD, where the authors did not consider the matrices of connections.

As we can see, our proposed method based on a matrix of connections provided as input to a CNN allows for more accurate results. This reinforces the importance of using a data set that encompasses the connections between brain regions. Indeed, the network structure is a fundamental ingredient to differentiate healthy individ-

uals from patients presenting neurological disorders, as verified in many papers (e.g. [24, 64–67]).

In Figures 4 we show the ROC curve for the best results, i.e. for AD (using Pearson's correlation) and SZ (using Granger causality test), respectively. For AD, the micro and macro-average ROC curve areas are 0.99 and 1.0, respectively, the micro and macro-average ROC curve areas are 0.92 for both cases. For comparison, Fig-

TABLE IV. Classification results for AD using the CNN_{tuned} model (best results are in bold).

Matrices of connections	Hyperparameter	Sample	Accuracy	Precision	Recall	AUC
Granger causality	Random	Train	0.81	0.81	0.81	0.88
	Search	Test	0.75	0.75	0.75	0.97
	hyper-band	Train	0.65	0.65	0.65	0.65
		Test	0.75	0.75	0.75	0.97
	Bayesian Optimization	Train	0.68	0.68	0.68	0.82
		Test	0.75	0.75	0.75	0.93
Pearson's correlation	Random	Train	0.95	0.95	0.95	0.98
	Search	Test	1.00	1.00	1.00	1.00
	hyper-band	Train	0.86	0.86	0.86	0.90
		Test	1.00	1.00	1.00	1.00
	Bayesian Optimization	Train	0.88	0.88	0.88	0.98
		Test	1.00	1.00	1.00	1.00
Spearman correlation	Random	Train	0.47	0.47	0.45	0.47
	Search	Test	0.75	0.75	0.75	0.75
	hyper-band	Train	0.47	0.47	0.47	0.45
		Test	0.75	0.75	0.75	0.62
	Bayesian Optimization	Train	0.47	0.47	0.47	0.45
		Test	0.75	0.75	0.75	0.68

TABLE V. Classification results for SZ using the CNN_{tuned} model (best results are in bold).

Matrices of connections	Hyperparameter	Sample	Accuracy	Precision	Recall	AUC
Granger causality	Random	Train	0.90	0.90	0.90	0.93
	Search	Test	1.00	1.00	1.00	1.00
	hyper-band	Train	0.73	0.73	0.73	0.77
		Test	0.72	0.72	0.72	0.78
	Bayesian Optimization	Train	0.72	0.72	0.72	0.78
		Test	1.00	1.00	1.00	1.00
Pearson's correlation	Random	Train	0.54	0.54	0.54	0.54
	Search	Test	0.50	0.50	0.50	0.50
	hyper-band	Train	0.54	0.54	0.54	0.54
		Test	0.50	0.50	0.50	0.50
	Bayesian Optimization	Train	0.54	0.54	0.54	0.54
		Test	0.50	0.50	0.50	0.50
Spearman correlation	Random	Train	0.53	0.53	0.53	0.53
	Search	Test	0.50	0.50	0.50	0.50
	hyper-band	Train	0.53	0.53	0.53	0.53
		Test	0.50	0.50	0.50	0.50
	Bayesian Optimization	Train	0.53	0.53	0.53	0.53
		Test	0.50	0.50	0.50	0.50

TABLE VI. Classification results for AD using the $CNN_{untuned}$ model (best results are in bold).

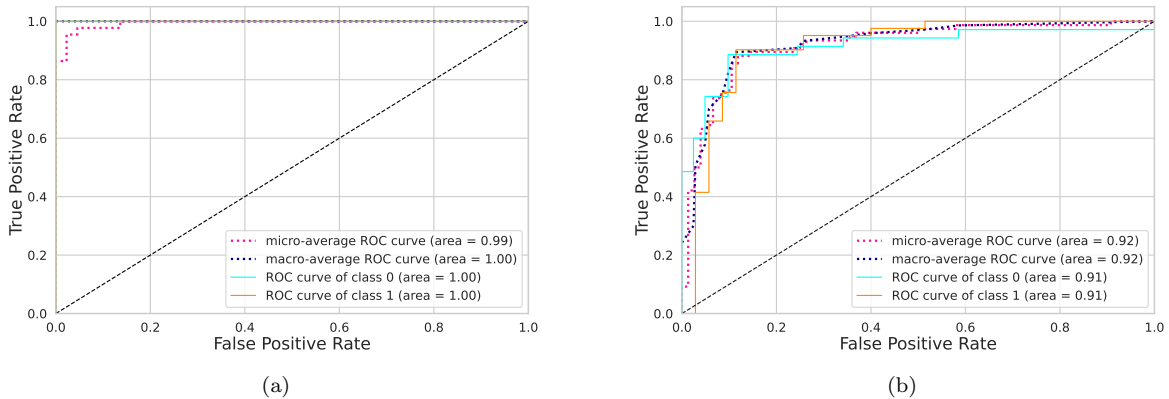
Matrices of connections	Sample	Accuracy	Precision	Recall	AUC
Granger causality	Train	0.97	0.97	0.99	0.99
	Test	0.58	0.57	0.66	0.75
Pearson's correlation	Train	0.98	0.99	0.98	0.99
	Test	0.92	1.00	0.83	1.00
Spearman's correlation	Train	0.97	0.98	0.97	0.99
	Test	0.83	1.00	0.66	1.00

ure 5 shows the ROC curve for AD and SZ using raw times series, where the micro and macro-average ROC curve areas are 0.75 for AD and around 0.55 for AZ. Comparing these results, we conclude that the use of the

matrix of connections provides the most accurate classifications.

TABLE VII. Classification results for SZ using the $CNN_{untuned}$ model.

Matrices of connections	Sample	Accuracy	Precision	Recall	AUC
Granger causality	Train	0.97	0.97	0.97	0.99
	Test	0.52	0.53	0.73	0.55
Pearson's correlation	Train	0.61	0.58	1.00	0.53
	Test	0.57	0.55	1.00	0.45
Spearman's correlation	Train	0.62	0.59	0.97	0.58
	Test	0.62	0.58	1.00	0.53

FIG. 4. ROC curve obtained from the CNN_{tuned} model. The matrices of connections are constructed by (a) Pearson's correlation for AD disease and (b) Granger causality for individuals diagnosed with SZ.TABLE VIII. Classification results for AD using raw EEG time series and the CNN_{tuned} model.

Set	Accuracy	Precision	Recall	AUC
Train	0.68	0.61	1.00	0.68
Test	0.75	0.66	1.00	0.75

TABLE IX. Classification results for SZ using raw EEG time series and the CNN_{tuned} model.

Set	Accuracy	Precision	Recall	AUC
Train	0.62	0.62	1.00	0.50
Test	0.55	0.55	1.00	0.50

V. CONCLUSION

In this paper, we propose a method for automatic diagnosis of AD and SZ based on EEG time series and deep learning. We infer the matrix of connections between brain areas following three different approaches, based on Granger causality, Pearson's and Spearman's correlations. These matrices are included in a convolutional neural network, tuned with the random search, hyperband, and Bayesian optimization. We verify that this approach provides a very accurate classification of patients with AD and SZ diseases. The comparison with the tra-

ditional method that considers raw EEG data shows that our method is more accurate, reinforcing the importance of network topology for the description of brain data. Our method is general and can be used for any mental disorder in which EEG times series can be recorded.

A limitation of our analysis is the relatively small data set, although this is common in other studies on disease classification [20]. However, even with this restriction, our algorithm worked very well, showing that AD and SZ are associate to changes in brain organization. As future work, we suggest to consider larger data sets and additional information about the patients, like health conditions and age. A method that provides the level of the evolution of the disease is also an interesting topic to be developed from our study.

VI. ACKNOWLEDGEMENTS

F.A.R. acknowledges CNPq (grant 309266/2019-0) and FAPESP (grant 19/23293-0) for the financial support given for this research. A.M.P. acknowledges FAPESP (grant 2019/22277-0) for the financial support given this research. K.R. acknowledges FAPESP grant 2019/26595-7. C.T. gratefully acknowledges financial support from the Zentrum für Wissenschaftliche Services und Transfer (ZeWiS) Aschaffenburg, Germany.

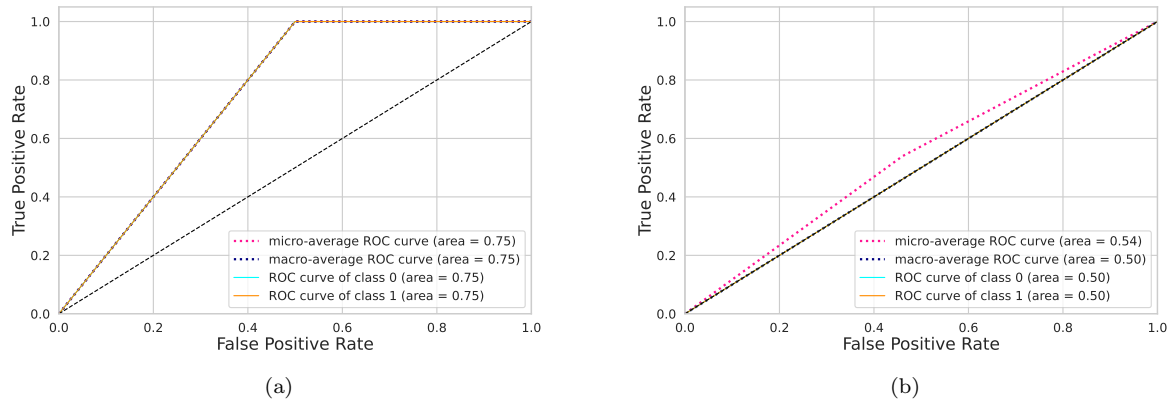


FIG. 5. ROC curve obtained from raw EEG time series for (a) individuals diagnosed with AD and (b) individuals with SZ.

- [1] W. H. Organization, *Neurological disorders: public health challenges* (World Health Organization, 2006).
- [2] E. Dolgin, How to defeat dementia, *Nature News* **539**, 156 (2016).
- [3] World Health Organization, <https://www.who.int/news-room/fact-sheets/detail/dementia> (2021), [Online; Accessed on September 21, 2021].
- [4] S. Rodriguez, C. Hug, P. Todorov, N. Moret, S. A. Boswell, K. Evans, G. Zhou, N. T. Johnson, B. T. Hyman, P. K. Sorger, *et al.*, Machine learning identifies candidates for drug repurposing in alzheimer's disease, *Nature Communications* **12**, 1 (2021).
- [5] V. Jahmunah, S. L. Oh, V. Rajinikanth, E. J. Ciaccio, K. H. Cheong, N. Arunkumar, and U. R. Acharya, Automated detection of schizophrenia using nonlinear signal processing methods, *Artificial intelligence in medicine* **100**, 101698 (2019).
- [6] I. I. Gottesman and J. Shields, *Schizophrenia* (CUP Archive, 1982).
- [7] World Health Organization, <https://www.who.int/news-room/fact-sheets/detail/schizophrenia> (2021), [Online; Accessed on September 21, 2021].
- [8] D. Borsboom and A. O. Cramer, Network analysis: an integrative approach to the structure of psychopathology, *Annual Review of Clinical Psychology* **9**, 91 (2013).
- [9] E. I. Fried, C. D. van Borkulo, A. O. Cramer, L. Boschloo, R. A. Schoevers, and D. Borsboom, Mental disorders as networks of problems: a review of recent insights, *Social Psychiatry and Psychiatric Epidemiology* **52**, 1 (2017).
- [10] D. Borsboom, Psychometric perspectives on diagnostic systems, *Journal of clinical psychology* **64**, 1089 (2008).
- [11] C. R. Jack Jr, V. J. Lowe, S. D. Weigand, H. J. Wiste, M. L. Senjem, D. S. Knopman, M. M. Shiung, J. L. Gunter, B. F. Boeve, B. J. Kemp, *et al.*, Serial pib and mri in normal, mild cognitive impairment and alzheimer's disease: implications for sequence of pathological events in alzheimer's disease, *Brain* **132**, 1355 (2009).
- [12] Y. Ding, J. H. Sohn, M. G. Kawczynski, H. Trivedi, R. Harnish, N. W. Jenkins, D. Lituiev, T. P. Copeland, M. S. Aboian, C. Mari Aparici, *et al.*, A deep learning model to predict a diagnosis of alzheimer disease by using 18f-fdg pet of the brain, *Radiology* **290**, 456 (2019).
- [13] K. Walhovd, A. Fjell, J. Brewer, L. McEvoy, C. Fennema-Notestine, D. Hagler, R. Jennings, D. Karow, A. Dale, A. D. N. Initiative, *et al.*, Combining mr imaging, positron-emission tomography, and csf biomarkers in the diagnosis and prognosis of alzheimer disease, *American Journal of Neuroradiology* **31**, 347 (2010).
- [14] A. Del Guerra, S. Ahmad, M. Avram, N. Belcari, A. Berneking, L. Biagi, M. G. Bisogni, F. Brandl, J. Cabello, N. Camarlinghi, *et al.*, Trimage: A dedicated trimodality (pet/mr/eeg) imaging tool for schizophrenia, *European Psychiatry* **50**, 7 (2018).
- [15] L. Tait, F. Tamagnini, G. Stothart, E. Barvas, C. Monaldini, R. Frusciante, M. Volpini, S. Guttmann, E. Coulthard, J. T. Brown, *et al.*, Eeg microstate complexity for aiding early diagnosis of alzheimer's disease, *Scientific Reports* **10**, 1 (2020).
- [16] L. R. Trambaiolli, T. H. Falk, F. J. Fraga, R. Anghinah, and A. C. Lorena, Eeg spectro-temporal modulation energy: a new feature for automated diagnosis of alzheimer's disease, in *2011 Annual International Conference of the IEEE Engineering in Medicine and Biology Society (IEEE, 2011)* pp. 3828–3831.
- [17] T. H. Falk, F. J. Fraga, L. Trambaiolli, and R. Anghinah, Eeg amplitude modulation analysis for semi-automated diagnosis of alzheimer's disease, *EURASIP Journal on Advances in Signal Processing* **2012**, 1 (2012).
- [18] L. Piubelli, L. Pollegioni, V. Rabattoni, M. Mauri, L. P. Cariddi, M. Versino, and S. Sacchi, Serum d-serine levels are altered in early phases of alzheimer's disease: towards a precocious biomarker, *Translational Psychiatry* **11**, 1 (2021).
- [19] A. M. Pineda, F. M. Ramos, L. E. Betting, and A. S. Campanharo, Quantile graphs for eeg-based diagnosis of alzheimer's disease, *Plos One* **15**, e0231169 (2020).
- [20] S. L. Oh, J. Vicnesh, E. J. Ciaccio, R. Yuvaraj, and U. R. Acharya, Deep convolutional neural network model for automated diagnosis of schizophrenia using eeg signals,

- Applied Sciences **9**, 2870 (2019).
- [21] M. Ahmadlou, H. Adeli, and A. Adeli, Fractality and a wavelet-chaos-methodology for eeg-based diagnosis of alzheimer disease, *Alzheimer Disease & Associated Disorders* **25**, 85 (2011).
- [22] R. Buettner, D. Beil, S. Scholtz, and A. Djemai, Development of a machine learning based algorithm to accurately detect schizophrenia based on one-minute eeg recordings, in *Proceedings of the 53rd Hawaii International Conference on System Sciences* (2020).
- [23] O. Sporns, Network analysis, complexity, and brain function, *Complexity* **8**, 56 (2002).
- [24] G. F. de Arruda, L. da Fontoura Costa, D. Schubert, and F. A. Rodrigues, Structure and dynamics of functional networks in child-onset schizophrenia, *Clinical Neurophysiology* **125**, 1589 (2014).
- [25] L. d. F. Costa, F. A. Rodrigues, G. Travieso, and P. R. Villas Boas, Characterization of complex networks: A survey of measurements, *Advances in Physics* **56**, 167 (2007).
- [26] L. da F Costa, P. V. Boas, F. Silva, and F. Rodrigues, A pattern recognition approach to complex networks, *Journal of Statistical Mechanics: Theory and Experiment* **2010**, P11015 (2010).
- [27] M. Diykh, Y. Li, and P. Wen, Classify epileptic eeg signals using weighted complex networks based community structure detection, *Expert Systems with Applications* **90**, 87 (2017).
- [28] I. Goodfellow, Y. Bengio, and A. Courville, *Deep learning* (MIT press, 2016).
- [29] U. R. Acharya, S. L. Oh, Y. Hagiwara, J. H. Tan, and H. Adeli, Deep convolutional neural network for the automated detection and diagnosis of seizure using eeg signals, *Computers in Biology and Medicine* **100**, 270 (2018).
- [30] K. Kashiparekh, J. Narwariya, P. Malhotra, L. Vig, and G. Shroff, ConvTimentet: A pre-trained deep convolutional neural network for time series classification, in *2019 International Joint Conference on Neural Networks (IJCNN)* (IEEE, 2019) pp. 1–8.
- [31] J. Islam and Y. Zhang, Brain mri analysis for alzheimer’s disease diagnosis using an ensemble system of deep convolutional neural networks, *Brain informatics* **5**, 1 (2018).
- [32] A. Duneja, T. Puyalnithi, M. V. Vankadara, and N. Chilamkurti, Analysis of inter-concept dependencies in disease diagnostic cognitive maps using recurrent neural network and genetic algorithms in time series clinical data for targeted treatment, *Journal of Ambient Intelligence and Humanized Computing* **10**, 3915 (2019).
- [33] U. R. Acharya, S. L. Oh, Y. Hagiwara, J. H. Tan, H. Adeli, and D. P. Subha, Automated eeg-based screening of depression using deep convolutional neural network, *Computer Methods and Programs in Biomedicine* **161**, 103 (2018).
- [34] S. L. Oh, Y. Hagiwara, U. Raghavendra, R. Yuvaraj, N. Arunkumar, M. Murugappan, and U. R. Acharya, A deep learning approach for parkinson’s disease diagnosis from eeg signals, *Neural Computing and Applications* , 1 (2018).
- [35] Ö. Yıldırım, U. B. Baloglu, and U. R. Acharya, A deep convolutional neural network model for automated identification of abnormal eeg signals, *Neural Computing and Applications* , 1 (2018).
- [36] A. M. Bastos and J.-M. Schoffelen, A tutorial review of functional connectivity analysis methods and their interpretational pitfalls, *Frontiers in Systems Neuroscience* **9**, 175 (2016).
- [37] A. K. Seth, A. B. Barrett, and L. Barnett, Granger causality analysis in neuroscience and neuroimaging, *Journal of Neuroscience* **35**, 3293 (2015).
- [38] J. Bonita, L. Ambolode, B. Rosenberg, C. Cellucci, T. Watanabe, P. Rapp, and A. Albano, Time domain measures of inter-channel eeg correlations: a comparison of linear, nonparametric and nonlinear measures, *Cognitive neurodynamics* **8**, 1 (2014).
- [39] W. S. Pritchard, D. W. Duke, and K. L. Coburn, Altered eeg dynamical responsivity associated with normal aging and probable alzheimer’s disease, *Dementia and Geriatric Cognitive Disorders* **2**, 102 (1991).
- [40] S. F. Timashev, O. Y. Panischev, Y. S. Polyakov, S. A. Demin, and A. Y. Kaplan, Analysis of cross-correlations in electroencephalogram signals as an approach to proactive diagnosis of schizophrenia, *Physica A: Statistical Mechanics and its Applications* **391**, 1179 (2012).
- [41] C. W. Granger, Investigating causal relations by econometric models and cross-spectral methods, *Econometrica: journal of the Econometric Society* , 424 (1969).
- [42] J. Benesty, J. Chen, Y. Huang, and I. Cohen, Pearson correlation coefficient, in *Noise reduction in speech processing* (Springer, 2009) pp. 1–4.
- [43] D. Lubinski, Introduction to the special section on cognitive abilities: 100 years after spearman’s (1904)”’general intelligence,’objectively determined and measured” ., *Journal of personality and social psychology* **86**, 96 (2004).
- [44] C. H. Comin, T. Peron, F. N. Silva, D. R. Amancio, F. A. Rodrigues, and L. d. F. Costa, Complex systems: Features, similarity and connectivity, *Physics Reports* **861**, 1 (2020).
- [45] S. G. Shandilya and M. Timme, Inferring network topology from complex dynamics, *New Journal of Physics* **13**, 013004 (2011).
- [46] B. Lusch, P. D. Maia, and J. N. Kutz, Inferring connectivity in networked dynamical systems: Challenges using granger causality, *Physical Review E* **94**, 032220 (2016).
- [47] F. Millstein, *Convolutional Neural Networks In Python: Beginner’s Guide To Convolutional Neural Networks In Python* (Frank Millstein, 2020).
- [48] D. H. Hubel and T. N. Wiesel, Receptive fields, binocular interaction and functional architecture in the cat’s visual cortex, *The Journal of Physiology* **160**, 106 (1962).
- [49] G. López-Risueño, J. Grajal, S. Haykin, and R. Díaz-Oliver, Convolutional neural networks for radar detection, in *International Conference on Artificial Neural Networks* (Springer, 2002) pp. 1150–1155.
- [50] Y. LeCun *et al.*, Generalization and network design strategies, *Connectionism in perspective* **19**, 143 (1989).
- [51] Y. LeCun, Y. Bengio, and G. Hinton, Deep learning, *Nature* **521**, 436 (2015).
- [52] F. Hutter, J. Lücke, and L. Schmidt-Thieme, Beyond manual tuning of hyperparameters, *KI-Künstliche Intelligenz* **29**, 329 (2015).
- [53] J. Bergstra and Y. Bengio, Random search for hyperparameter optimization., *Journal of Machine Learning Research* **13** (2012).
- [54] A. Rostamizadeh, A. Talwalkar, G. DeSalvo, K. Jamieson, and L. Li, Efficient hyperparameter

- optimization and infinitely many armed bandits, in *5th International Conference on Learning Representations* (2017).
- [55] P. Doke, D. Shrivastava, C. Pan, Q. Zhou, and Y.-D. Zhang, Using cnn with bayesian optimization to identify cerebral micro-bleeds, *Machine Vision and Applications* **31**, 1 (2020).
- [56] N. Srivastava, G. Hinton, A. Krizhevsky, I. Sutskever, and R. Salakhutdinov, Dropout: a simple way to prevent neural networks from overfitting, *The journal of machine learning research* **15**, 1929 (2014).
- [57] O. Maimon and L. Rokach, *Data Mining and Knowledge Discovery Handbook* (Springer Science & Business Media, 2010).
- [58] J. Huang and C. X. Ling, Using auc and accuracy in evaluating learning algorithms, *IEEE Transactions on Knowledge and Data Engineering* **17**, 299 (2005).
- [59] A. Ozcift and A. Gulten, Classifier ensemble construction with rotation forest to improve medical diagnosis performance of machine learning algorithms, *Computer methods and programs in biomedicine* **104**, 443 (2011).
- [60] L. Shen, H. Chen, Z. Yu, W. Kang, B. Zhang, H. Li, B. Yang, and D. Liu, Evolving support vector machines using fruit fly optimization for medical data classification, *Knowledge-Based Systems* **96**, 61 (2016).
- [61] A. K. Tanwani, J. Afridi, M. Z. Shafiq, and M. Farooq, Guidelines to select machine learning scheme for classification of biomedical datasets, in *European Conference on Evolutionary Computation, Machine Learning and Data Mining in Bioinformatics* (Springer, 2009) pp. 128–139.
- [62] L. Nanni, A. Lumini, and S. Brahnam, Local binary patterns variants as texture descriptors for medical image analysis, *Artificial intelligence in medicine* **49**, 117 (2010).
- [63] R. Janghel and Y. Rathore, Deep convolution neural network based system for early diagnosis of alzheimer’s disease, *IRBM* **42**, 258 (2021).
- [64] C. W. Lynn and D. S. Bassett, The physics of brain network structure, function and control, *Nature Reviews Physics* **1**, 318 (2019).
- [65] F. D. V. Fallani, F. A. Rodrigues, L. da Fontoura Costa, L. Astolfi, F. Cincotti, D. Mattia, S. Salinari, and F. Babiloni, Multiple pathways analysis of brain functional networks from eeg signals: an application to real data, *Brain Topography* **23**, 344 (2011).
- [66] F. A. Rodrigues and L. da Fontoura Costa, A structure–dynamic approach to cortical organization: Number of paths and accessibility, *Journal of Neuroscience Methods* **183**, 57 (2009).
- [67] L. Antigueira, F. A. Rodrigues, B. C. van Wijk, L. d. F. Costa, and A. Daffertshofer, Estimating complex cortical networks via surface recordings—a critical note, *Neuroimage* **53**, 439 (2010).